The American Journal of Pathology, Vol. 174, No. 2, February 2009

DOI: 10.2353/ajpath.2009.080598

Immunopathology and Infectious Diseases

IL-4/IL-13-Dependent Alternative Activation of Macrophages but Not Microglial Cells Is Associated with Uncontrolled Cerebral Cryptococcosis

Werner Stenzel,* Uwe Müller,†‡ Gabriele Köhler,§ Frank L. Heppner,* Manfred Blessing,†‡ Andrew N.J. McKenzie,¶ Frank Brombacher,‖ and Gottfried Alber†

From the Department of Neuropathology, Charité Universitätsmedizin, Berlin, Germany; the Institute of Immunology,† College of Veterinary Medicine, and the Molecular Pathogenesis Group,‡ Center for Biotechnology and Biomedicine, University of Leipzig, Leipzig, Germany; the Gerhard Domagk Institute for Pathology,§ University of Münster, Münster, Germany; the Medical Research Council Laboratory of Molecular Biology,¶ Cambridge, United Kingdom; the Institute of Infectious Disease and Molecular Medicine and International Centre for Genetic Engineering and Biotechnology,‖ University of Cape Town, Cape Town, South Africa*

Both interleukin (IL)-4- and IL-13-dependent Th2-mediated immune mechanisms exacerbate murine *Cryptococcus neoformans*-induced bronchopulmonary disease. To study the roles of IL-4 and IL-13 in cerebral cryptococcosis, IL-4 receptor α-deficient (IL-4Rα$^{-/-}$), IL-4-deficient (IL-4$^{-/-}$), IL-13-deficient (IL-13$^{-/-}$), IL-13 transgenic (IL-13$^{T/+}$), and wild-type mice were infected intranasally. IL-13$^{T/+}$ mice displayed a higher fungal brain burden than wild-type mice, whereas the brain burdens of IL-4Rα$^{-/-}$, IL-4$^{-/-}$, and IL-13$^{-/-}$ mice were significantly lower as compared with wild-type mice. On infection, 68% of wild-type mice and 88% of IL-13-overexpressing IL-13$^{T/+}$ mice developed significant cerebral lesions. In contrast, only a few IL-4Rα$^{-/-}$, IL-4$^{-/-}$, and IL-13$^{-/-}$ mice had small lesions in their brains. Furthermore, IL-13$^{T/+}$ mice harbored large pseudocystic lesions in the central nervous system parenchyma, bordered by voluminous foamy alternatively activated macrophages (aaMphs) that contained intracellular cryptococci, without significant microglial activation. In wild-type mice, aaMphs tightly bordered pseudocystic lesions as well, and these mice, in addition, showed microglial cell activation. Interestingly, in resistant IL-4$^{-/-}$, IL-13$^{-/-}$, and IL-4Rα$^{-/-}$ mice, no aaMphs were discernible. Microglial cells of all mouse genotypes neither internalized cryptococci nor expressed markers of alternative activation, although they displayed similar IL-4Rα expression levels as macrophages. These data provide the first evidence of the development of aaMphs in a central nervous system infectious disease model, pointing to distinct roles of macrophages versus microglial cells in the central nervous system immune response against *C. neoformans*. *(Am J Pathol 2009, 174:486–496; DOI: 10.2353/ajpath.2009.080598)*

The opportunistic pathogenic yeast *Cryptococcus neoformans* causes life-threatening fungal infections of most internal organs including the central nervous system (CNS), primarily in patients affected by immunodeficiency syndromes such as AIDS.[1] The pathogenesis of cryptococcosis is not fully understood, however, especially in cases of different levels of immunocompetence. It is generally accepted that the fungus first invades the respiratory system, where it leads to relatively mild or asymptomatic bronchopneumonia in the immunocompetent.[2–5] Fungemia with generalization of the infection may result from reduced immunological control mechanisms.[6–9] Invasion of the CNS with subsequent development of meningoencephalitis is the major cause of death during cryptococcosis.[10,11]

The precise reaction pattern of recruited inflammatory cells, especially monocytes/macrophages, due to fungal invasion of the CNS parenchyma has been addressed

Supported by research grants to W.S. (Köln Fortune grants 85/2006 & 76/2007), to G.A. (Deutsche Forschungsgemeinschaft grant AL 371/5-2); Federal Ministry for Economic Co-operation and Development for a research project with F.B. (grant AL 371/5-3), and to G.K. (Rolf-Dierichs-Stiftung, Münster, Germany).

W.S. and U.M. contributed equally to this work.

Accepted for publication October 24, 2008.

Supplemental material for this article can be found on *http://ajp.amjpathol.org*.

Address reprint requests to Dr. Werner Stenzel, Institute of Neuropathology, Charité Universitätsmedizin, Augustenburger Platz 1, 13353 Berlin, Germany. E-mail: werner.stenzel@charite.de.

mainly via analysis of helper T cell (Th)1 responses.[12] In this context, in addition to protective Th1-driven immune responses, the role of Th2 cytokines has gained interest recently.[13] The major Th2 cytokines interleukin (IL)-4 and IL-13 act via the IL-4Rα chain together with the γ_c chain or the IL-13Rα1/2 chains, and regulate macrophage functional status.[14] IL-4 has been shown to be detrimental in murine models of systemic and pulmonary cryptococcosis,[6,15–18] and we have recently illustrated the role of IL-13 in inducing the formation of alternatively activated macrophages (aaMphs) in murine pulmonary cryptococcosis.[19]

The activation phenotype of macrophages may critically influence the regulatory mechanisms by which inflammation and infection in the CNS are controlled. According to the current paradigm, classically activated macrophages are primed by interferon-γ and produce tumor necrosis factor, IL-1, oxygen and nitrogen radicals,[20] thereby producing proinflammatory cytokines that regulate the Th1 immune response. In contrast, aaMph[21] develop in response to Th2 cytokine stimulation such as IL-4 and IL-13 and are characterized by expression of genes associated with endocytosis and tissue repair such as arginase-1, mannose receptor (CD206), found-in-inflammatory-zone (FIZZ), and chitinase 3-like 3 (YM1) and largely fail to produce nitric oxide (NO) due to their induction of arginase.[22] As such, they are thought to be involved in tissue repair and remodeling,[22,23] in protection against diet-induced obesity,[24,25] and schistosomiasis,[26] but they may also elicit adverse tissue processes such as pulmonary or liver fibrosis.[27–31] In particular, their development renders the host vulnerable to infection with pathogens where macrophage activation and killing functions are required.[32]

In murine models of pulmonary *C. neoformans* infection, aaMph have been shown to be associated with uncontrolled lung infection.[18,19] The role of aaMph versus classically activated macrophage in the CNS due to pulmonary infection with the neurotropic pathogen *C. neoformans* has not been defined yet. In this study, we aimed to characterize the morphology and functional status of CNS macrophages in cerebral cryptococcosis following intranasal infection of susceptible wild-type and IL-13-transgenic BALB/c mice. Moreover, using mice unable to produce IL-4 or IL-13 or respond to both (IL-4R$\alpha^{-/-}$ mice), we show that abrogation of CNS aaMph development is associated with controlled infection.

Materials and Methods

Mice

Six to ten-week-old female wild-type, IL-4R$\alpha^{-/-}$,[33] IL-4$^{-/-}$,[34] IL-13$^{-/-}$,[35] as well as IL-13$^{T/+}$,[36] mice on BALB/c background were maintained in an IVC-Caging system under specific pathogen-free conditions and in accordance with the guidelines approved by the Animal Care and Usage Committee of the 'Regierungspräsidium Leipzig.' Sterile food and water were given *ad libitum*. The mice were tested periodically for pathogens in accordance with the recommendations for health monitoring of mice provided by the Federation of European Laboratory Animal Science Associations (FELASA) accreditation board. All mice were tested negative for pinworms and other endo- and ectoparasites.

Intranasal Infection of Mice with C. neoformans

Encapsulated *C. neoformans*, strain 1841, serotype D was kept as a frozen stock in skim milk and was grown in Sabouraud dextrose medium (2% glucose, 1% peptone, Sigma, Deisenhofen, Germany) overnight on a shaker at 30°C. Cells were washed twice in sterile PBS, resuspended in PBS, and counted in a hematocytometer. Inocula were diluted in PBS to a concentration of 2.5×10^4/ml for intranasal (i.n.) injections. Mice were infected by i.n. application of 10 μl volumes per nostril containing a total of 500 colony-forming units. For the intranasal infection, mice were anesthetized i.p. with a 1:1 mixture of 10% ketamine (100 mg/ml; Ceva Tiergesundheit, Düsseldorf, Germany) and 2% xylazine (20 mg/ml; Ceva Tiergesundheit).

Determination of Survival Rate and CNS Fungal Burden

Infected mice were monitored daily for survival and morbidity. Fungal burden was determined after sterile removal of the CNS from sacrificed mice and homogenization in 1 ml PBS with an Ultra-Turrax (T8; IKA-Werke, Staufen, Germany). Serial dilutions of the homogenates were plated on Sabouraud dextrose agar plates and colonies were counted after an incubation period of 72 hours at 30°C.

CNS Tissue Processing for Immunohistological Analysis and Electron Microscopy

On the indicated days post infection (p.i.), *C. neoformans*-infected wild-type, IL-4R$\alpha^{-/-}$, IL-4$^{-/-}$, IL-13$^{-/-}$, and IL-13$^{T/+}$, or uninfected mice, were perfused intra-cardially with 0.9% saline under CO_2 asphyxia. The brains of the animals were sterilely removed, mounted on thick filter paper with Tissue Tek optimal cutting temperature compound (Miles Scientific, Naperville, IL), snap-frozen in isopentane (Fluka, Neu-Ulm, Germay) pre-cooled on dry ice, and stored at −80°C.

For immunohistochemistry, 10-μm frozen sections were prepared in a serial fashion (30 transversal sections on six consecutive levels per CNS). The following rat anti-mouse monoclonal antibodies, obtained as hybridomas from the ATCC (Manassas, VA), were used for staining procedures: CD4 (clone G.K.1.5), CD8 (clone 2.43), CD45 (LCA, clone M1/9.3.4.HL.2), F4/80 (F4/80), MHC class II (I-A^{b,d,q} haplotypes, clone M5.114.15.2), and Ly6-G (GR1; clone RB6−8C5). Additionally, CD206 (mannose receptor) rat anti-mouse antibody (Serono, Unterschleißheim, Germany) and YM1 (ECF-L) goat anti-

mouse antibody (R&D Systems, Minneapolis, MN) were used for staining of alternatively activated macrophages.

Immunohistochemistry was performed by use of the Vectastain Elite ABC-Kit (Vector, Burlingame, CA) with appropriate biotinylated secondary antibodies. The peroxidase reaction product was visualized using 3,3′-diaminobenzidine (Sigma) as chromogene and H_2O_2 as cosubstrate. Negative controls, without application of the primary antibody, confirmed the specificity of the reactions. Glucuronoxylomannan (GXM) immunostaining was performed using mab 18B7 (kindly provided by Dr. Arturo Casadevall, Albert Einstein College of Medicine, New York, NY), and the Vector MOM Fluoresceine KIT (Vector). Histopathological alterations were microscopically evaluated on H&E-stained, and immunostained horizontal brain sections. The samples prepared for electron microscopy analysis were fixed in 2.5% cacodylate-buffered glutaraldehyde (pH 7.35). Following postfixation in phosphate-buffered 1.3% osmium tetroxide, the tissues were rinsed in buffer, dehydrated in graded alcohols and processed into polymerized blocks of Epon resin. Sections for initial light microscopy to determine tissue quality and architecture suitable for ultrastructure were cut at 0.5 μm and stained with toluidine blue. For electron microscopy, thin sections were cut with a diamond knife, mounted on copper grids, stained with alkaline lead citrate and 8% uranyl acetate, and examined using a Philips EM 208 electron microscope (Philips, Eindhoven, The Netherlands) operating at 80 kV. Photography was performed with a Morada digital camera (Olympus SIS, Munster, Germany).

RNA Extraction

Total RNA was extracted from brain tissue samples of the respective time points using the trizol/chloroform method according to the manufacturer's instruction (Invitrogen Carlsbad, CA), and resuspended in 60 μl DEPC-treated water. The concentration of total RNA was determined using the Qubit fluorometer according to the manufacturer's protocol (Invitrogen, Eugene, OR).

Quantitative Real-Time PCR

The RNA was reverse transcribed using the High-Capacity cDNA Archive Kit (Applied Biosystems, Foster City, CA) according to the manufacturer's protocol using 1 ng total RNA per sample as described.[37] Briefly, the expression level of arginase-1, YM1, and the endogenous control gene, hypoxanthin-guanine-phosphoribosyl-transferase (*hprt*), in the specimens was analyzed by real-time quantitative reverse transcriptase (RT)-PCR using the 5′-nuclease technology on an ABI PRISM 7300HT Sequence Detection System and the Mouse TaqMan pre-developed assay reagents (both: Applied Biosystems). The assay identification numbers are as follows: IL-4, Mm00445259_m1; IL-13, Mm00434204_m1; Arginase-1, Mm01190441_g1; YM1, Mm00657889_mH, and hypoxanthine-guanine-phosphoribosyl-transferase (HPRT), Mm00446968_m1. PCR reactions were prepared in a final volume of 20 μl, with final concentrations of 1x TaqMan Universal PCR Master Mix (Applied Biosystems), and a cDNA equivalent of 5 ng RNA. All analyses were performed in triplicate, and the threshold cycle (C_t) was determined. Gene expression was concomitantly measured in naive (non infected) murine brain as calibrator, to allow comparison between five different samples of wild-type, IL-4R$\alpha^{-/-}$, IL-4$^{-/-}$, IL-13$^{-/-}$, and IL-13$^{T/+}$ mice, using the $\Delta\Delta C_t$-method.[38]

Cytokine and Antibody Analysis

Cytokine concentrations were determined by sandwich enzyme-linked immunosorbent assay systems with unlabeled capture antibodies (Abs), and labeled detection Abs. To determine the concentration of IL-4, mAb 11B11 was used as the capture Ab and biotin-labeled BVD6-24G2 (BD Pharmingen) was used as the detection Ab followed by incubation with peroxidase-labeled streptavidin. The concentration of IL-13 was detected with the R&D Systems Duoset kit.

Flow Cytometry

Cerebral leukocytes were isolated from brains after perfusion with 0.9% NaCl. Brain tissue was minced through a 100 μm-mesh sieve Becton-Dickcinson (BD), leukocytes were separated by Percoll gradient centrifugation (Amersham-Pharmacia, Freiburg, Germany),[39] and brain-derived leukocytes were subjected to double or triple immunofluorescence staining followed by flow cytometry as described.[37,40] Macrophages were distinguished from microglial cells according to their higher levels of CD45.[41] Neutrophils, which were LCA^{high}Gr-1^{high}, could be distinguished from macrophages (LCA^{high}Gr-1^{-} and LCA^{high}Gr-1^{dim}). The expression level of IL-4Rα on cells was analyzed by using a biotinylated antibody against murine CD124 (clone mIL4R-M1; BD), combined with streptavidin-allophycocyanine. Brains of 5 mice were cut into halves, while 1 ml of each 5 halves were pooled and subjected to flow cytometry, the other 5 halves were cryopreserved individually. Before pooling these halves, 1 ml of the homogenized brain tissue (each half was passed through a 100 μm sieve [BD] and suspended in 2 ml of PBS) was subjected to colony forming units analysis.

Statistical Evaluation

The one-tailed Mann-Whitney test was performed to determine the significance of differences in the intracerebral fungal load, and the two-tailed Mann-Whitney test for the number of intracerebral leukocytes between wild-type, IL-4R$\alpha^{-/-}$, IL-4$^{-/-}$, IL-13$^{-/-}$, and IL-13$^{T/+}$ mice, and quantitative differences in mRNA transcripts. Data are presented as means ± SD. The level of confidence for significance was $P < 0.05$. All experiments were performed in triplicate. A representative experiment is shown in each figure.

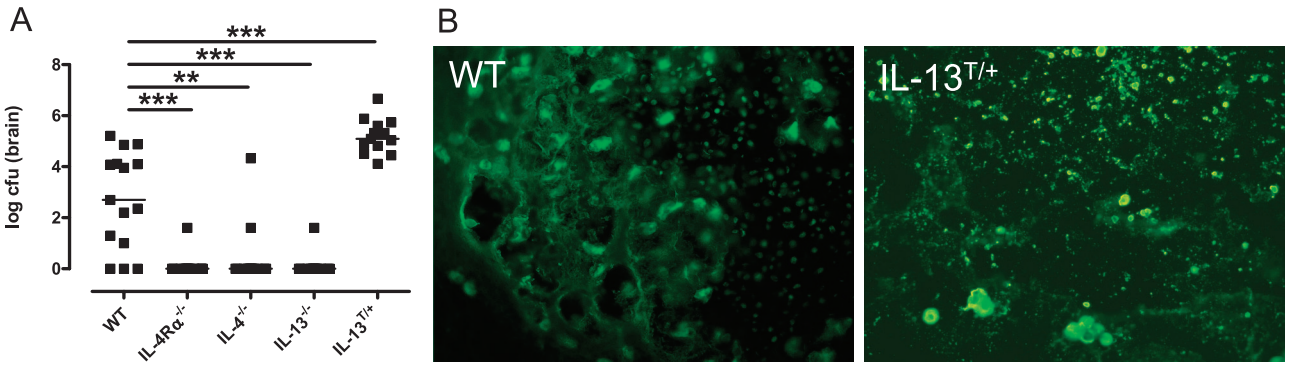

Figure 1. IL-4/IL-13 expression leads to elevated intracerebral fungal load in mice infected i.n. with *C. neoformans* for 60 days. **A:** The intracerebral fungal load of wild-type (WT), IL-4Rα$^{-/-}$, IL-4$^{-/-}$, IL-13$^{-/-}$, and IL-13$^{T/+}$ mice was counted after sterile removal of the brain (n = 5 animals/genotype) and data from four experiments were pooled. Data represent the median of 15 animals per group. Statistical analysis between wild-type, IL-4Rα$^{-/-}$, IL-4$^{-/-}$, IL-13$^{-/-}$, and IL-13$^{T/+}$ mice was performed by use of the Mann-Whitney-U Test. $^{**}P < 0.01$; $^{***}P < 0.001$. **B:** In wild-type mice, huge amounts of anti-GXM positive cryptococci and yeast fragments can be found within a pseudocystic lesion. In IL-13$^{T/+}$ mice, a large pseudocystic lesion, harboring densely packed masses of small yeast fragments, and large grouped intact yeasts are shown. Day 60 p.i.; Anti-GXM immunostaining magnification = original ×400.

Results

Elevated Cerebral Fungal Load in the Presence of IL-4 and IL-13 in Mice Infected Intranasally with C. neoformans *for 60 Days*

Following pulmonary infection of wild-type and the type 2 cytokine mutant mice, IL-4Rα$^{-/-}$, IL-4$^{-/-}$, IL-13$^{-/-}$, and IL-13$^{T/+}$ mice, with the highly virulent strain *C. neoformans* 1841, dissemination to the CNS becomes detectable after about 40 to 50 days of infection. At 60 dpi the expression of IL-4 or IL-13 in wild-type mice is associated with high organ burdens of *C. neoformans* within the CNS, and over-expression of IL-13 in IL-13$^{T/+}$ mice leads to even higher levels of cryptococci (Figure 1A). In contrast, brain infection was undetectable in almost all of the intranasally infected IL-4Rα$^{-/-}$, IL-4$^{-/-}$, and IL-13$^{-/-}$ mice, indicating protection from cerebral cryptococcosis in the absence of IL-4/IL-13 signaling (Figure 1A).

As shown in Figure 1B, deposition of the polysaccharide GXM associated with the capsule of *C. neoformans* was found abundantly in wild-type and IL-13$^{T/+}$ mice. In wild-type mice (Figure 1B), GXM-positive cryptococci were mostly found intact at the border of the lesion and fragmented within the center of the lesion. In IL-13$^{T/+}$ mice (Figure 1B), intense GXM immunostaining revealed a fragmented pattern with only a few intact yeasts. However, GXM immunoreactivity was absent in resistant IL-4Rα$^{-/-}$ mice, highly restricted to local lesions in (2 out of 25) IL-4$^{-/-}$ mice, and minimal in one (out of 25) IL-13$^{-/-}$ mouse (data not shown).

IL-4 and IL-13 Profoundly Impact Lesion Development within the CNS Induced by C. neoformans

Eighty-eight percent (ie, 22 out of 25) of IL-13$^{T/+}$ mice and 68% (ie, 17 out of 25) of wild-type mice showed intracerebral lesions, while only in 4% (ie, 1 out of 25) of IL-4Rα$^{-/-}$ mice, 8% (ie, 2 out of 25) of IL-4$^{-/-}$ mice, and 4% (ie, 1 out of 25) of IL-13$^{-/-}$ mice focal CNS lesions were detectable. The morphological reaction pattern of intracerebral inflammation by *C. neoformans* differed fundamentally in the different mouse strains. IL-13$^{T/+}$ mice harbored larger lesions, which were less well demarcated and contained more fungi or fungal fragments in their brains as compared with wild-type mice (Figure 2, E versus A). In comparing the susceptible genotypes with the resistant genotypes, the lesions had a pseudocystic morphology (Figure 2, A and E). These pseudocystic lesions, harboring fungal accumulations, were diffusely disseminated in all regions of the CNS, including the

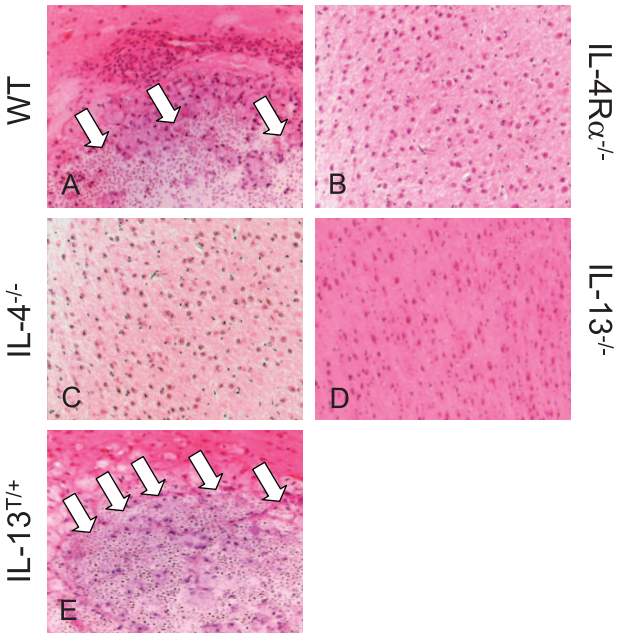

Figure 2. Development of pseudocystic lesion in large scale in the brains of susceptible *C. neoformans*-infected wild-type and IL-13$^{T/+}$ mice, but the absence of IL-4/−13 is associated with occasional formation of microglial nodules, granulomas, or only small pseudocystic lesions. Shown are representative micrographs (see supplemental figures). **A–E:** Day 60 pi; H&E staining of the brain of wild-type (WT), IL-4Rα$^{-/-}$, IL-4$^{-/-}$, IL-13$^{-/-}$, and IL-13$^{T/+}$ mice; magnification = original ×400. In wild-type and IL-13$^{T/+}$ mice large foamy macrophages bordering pseudocystic lesions filled with cryptococci (**white arrows**) could be found, whereas the brain parenchyma of IL-4Rα$^{-/-}$, IL-4$^{-/-}$, and IL-13$^{-/-}$ mice is unremarkable.

supratentorial lobes, the basal ganglia and the cerebellum in IL-13$^{T/+}$ mice. In contrast to IL-13$^{T/+}$ mice, in wild-type mice the semioval center white matter was exclusively affected. The CNS parenchyma of IL-4R$\alpha^{-/-}$ mice, IL-4$^{-/-}$ mice, and IL-13$^{-/-}$ mice was largely unremarkable (Figure 2, B–D). Two small microglial nodules were detected in the left frontal white matter in a single IL-4R$\alpha^{-/-}$ mouse, but fungal masses or fragments were consistently absent (supplemental Figure S1A, see *http://ajp.amjpathol.org*). In contrast, in two IL-4$^{-/-}$ mice (supplemental Figures S1B and S1C, see *http://ajp.amjpathol.org*), the lesion morphology was characterized by typical granuloma formation with significant accumulations of compact macrophages, with partial epitheloid appearance, and lymphocytes (supplemental Figure S1B, see *http://ajp.amjpathol.org*). Yeast accumulated focally in the center of the lesion but not in the cytoplasm of macrophages (supplemental Figure S1C, see *http://ajp.amjpathol.org*). In a single IL-13$^{-/-}$ mouse, a minor accumulation of *C. neoformans* within a small pseudocystic lesion was detected (supplemental Figure S1D, see *http://ajp.amjpathol.org*), while all of the other IL-13$^{-/-}$ mice did not show any inflammatory foci. *C. neoformans* mainly localized to the cytoplasm of macrophages situated at the border between CNS parenchyma and centrally pseudocystic lesion of wild-type and IL-13$^{T/+}$ mice (Figure 2, A and E). In comparison with the lung, where large encapsulated cryptococcal yeasts are detectable mainly extracellularly (Stenzel and Köhler, unpublished observation), huge masses of fungi and fungal fragments with variable size were apparently localized within the macrophages of the CNS in wild-type and IL-13$^{T/+}$ mice. Thus, expression of IL-4 and IL-13 correlates with loss of fungal control, and a specific reaction pattern of the CNS parenchyma leading to large pseudocystic lesions bordered by voluminous foamy macrophages filled with yeast. While the absence of IL-4 may rarely enable formation of granulomas, loss of IL-13 is associated with appearance of small pseudocystic lesions in rare cases, and concomitant loss of IL-4 and IL-13 signaling (ie, IL-4Rα deficiency) apparently suppresses cryptococcal invasion very effectively, with only scarce formation of microglial nodules.

In the Presence of IL-4 and IL-13, Elevated Numbers of Macrophages Rather than Microglial Cells in the Brain following Intranasal Infection with C. neoformans

Macrophages are central effector cells in cryptococcosis.[42] Quantitative analysis of brains by flow cytometry at day 60 p.i., revealed that CD11b^{+}CD45^{high} macrophages, and also Gr-1^{+}CD11b^{+}CD45^{high} neutrophils (data not shown), were found at the highest numbers in susceptible genotypes (ie, IL-13$^{T/+}$, and wild-type mice), whereas only low numbers of these cell types were found in IL-4R$\alpha^{-/-}$, IL-4$^{-/-}$, and IL-13$^{-/-}$ mice (Figure 3A). Following infection of mice with *C. neoformans,* it was specifically the number of macrophages that increased in

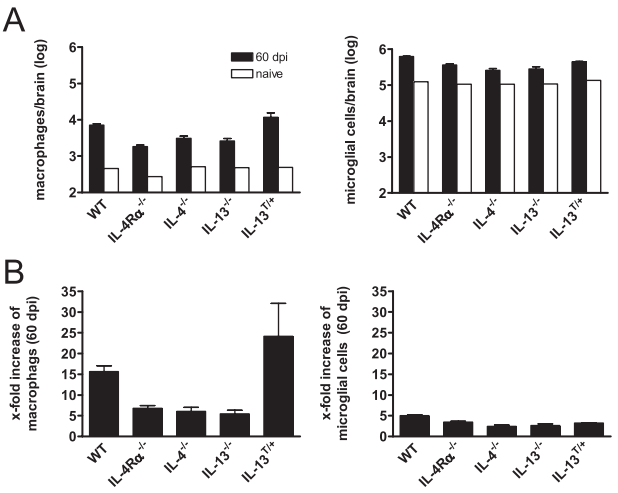

Figure 3. High numbers of macrophages infiltrate the CNS in the presence of IL-4/IL-13 following i.n. infection with *C. neoformans.* For fluorescence-activated cell sorting analysis of intracerebral leukocytes, brains of five mice per genotype were pooled following i.n. infection with *C. neoformans* in BALB/c wild-type (WT), IL-4R$\alpha^{-/-}$, IL-4$^{-/-}$, IL-13$^{-/-}$, and IL-13$^{T/+}$ mice (**A**). Three similar experiments from infected mice and one experiment from naïve mice are shown. Cells were isolated, stained for Gr-1, CD11b, CD45, and analyzed by flow cytometry. Data are expressed as numbers of cells of the respective cell type per brain. Numbers of the respective cell types of naïve mice are shown in open bars. In (**B**) the x-fold increase of macrophages and microglial cells during cryptococcosis (60 dpi) in comparison with naïve mice is shown.

brains of wild-type and IL-13$^{T/+}$ mice 15- and 24-fold, respectively. In contrast, there was only a relatively small increase in microglial cells (Figure 3B). Together, in susceptible IL-4 and IL-13 expressing wild-type and IL-13$^{T/+}$ mice, development of high cryptococcal burdens in the brain is associated with greatly enhanced numbers of macrophages but to a lesser degree with microglial cells.

In the Presence of IL-4 and IL-13, Large Foamy Macrophages Appear in the CNS after Cryptococcal Infection and Are, in Contrast to Microglial Cells, aaMphs

The CNS immune response to *C. neoformans* is primarily monocytic.[10,43] Moreover, in recent years classical versus alternative activation of macrophages have been shown to crucially affect the type of ensuing immune responses after infection.[22,24] In *C. neoformans* infection of the lung, development of aaMphs leads to increased mortality due to excessive immunopathology.[19,44,45] In light of elevated numbers of brain macrophages observed (Figure 3, A and B), we were interested in characterizing their activation status. Strikingly, in susceptible wild-type and IL-13$^{T/+}$ mice, large foamy macrophages strongly expressing CD206 and YM1 appeared (Figures 4 and 5). In parallel, expression of YM1, and less importantly arginase-1, mRNA was significantly elevated in the brains of infected wild-type and IL-13$^{T/+}$ mice (Figure 6). Numerous activated (ie, enlarged and ramified, see white arrow heads in Figure 4A) MHC class II microglial cells were detected in the vicinity of large pseudocystic lesions of wild-type mice. However, microglial cells were

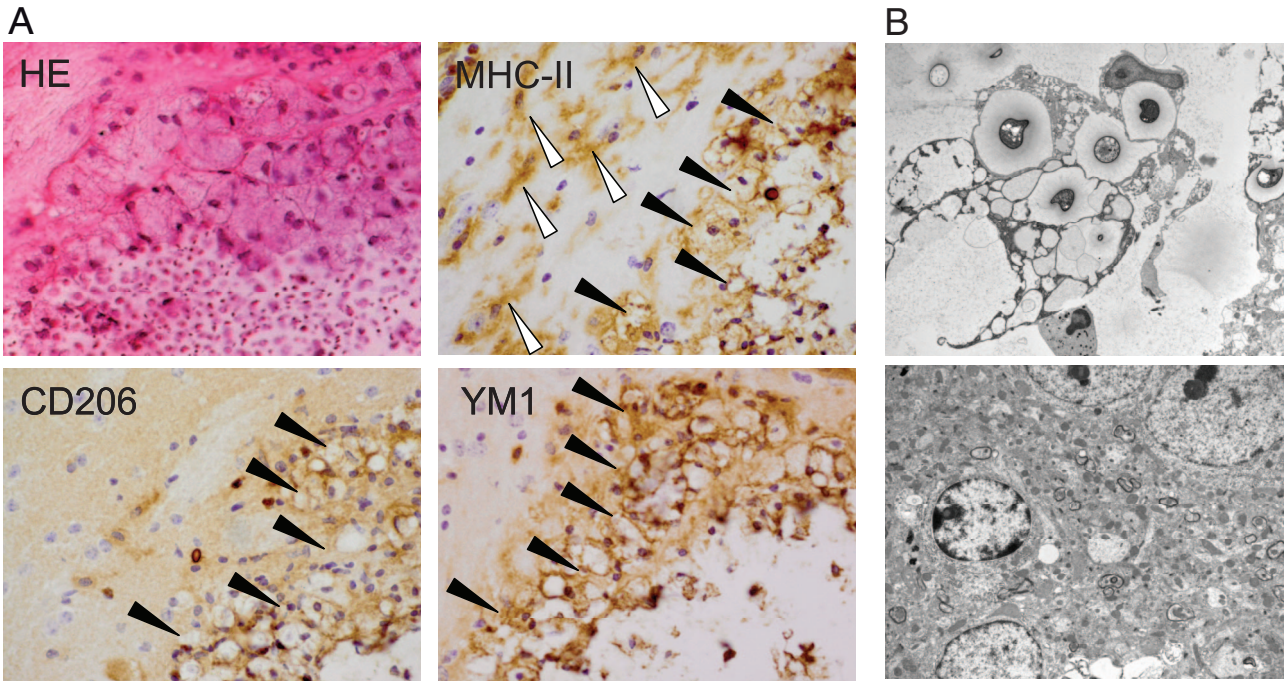

Figure 4. In the presence of IL-4 and IL-13, macrophages but not microglial cells expressing markers of alternative activation are detected in the brains of susceptible BALB/c wild-type mice at 60 d.p.i. **A:** Wild-type (WT) mice show that large pseudocystic lesion, harboring many small yeasts and yeast fragments, is bordered by inflammatory leukocytes, consisting mainly of large rounded foamy macrophages (**black arrowheads**). H&E staining, magnification = original ×600. The large foamy rounded cells are identified as MHC class II$^+$ macrophages tightly bordering the lesion. Activated MHC class II$^+$ ramified microglial cells (**white arrowheads**) are demonstrated in the outer vicinity of the lesion. Anti-MHC class II immunostaining, magnification = original ×600. Large round cells strongly express the CD206 antibody, whereas the antibody against the mannose receptor did not detect ramified microglial cells. Anti-CD206 immunostaining; magnification = original ×600. Many round cells, but not microglial cells, bordering the lesion strongly express the YM1 antibody. Anti-YM1 immunostaining; magnification = original ×600. **B: Upper panel:** Ultrastructural analysis of the identified type of macrophages reveals that they harbor yeasts and yeast fragments within their cytoplasm, and that they also contain numerous small vacuoles corresponding to their 'foamy' appearance, which are phagolysosomes. **Lower panel:** The ultrastructural analysis of microglial cells identifies a cell with dense-staining nucleus and marginated chromatin free of cryptococci or vacuolated lysosomes. Electron microscopy; magnification = original ×3000.

not found to express markers of alternative activation in this specific localization, indicating that the development of alternatively activated cells is restricted to macrophages but not microglial cells. The particular morphology of the large foamy macrophages was further characterized by electron microscopy of typical lesions found in wild-type mice (Figure 4B, upper panel). The electron micrograph demonstrates a giant foamy macrophage with intracellular yeasts also containing intracellular vacuoles. In contrast, microglial cells of the same animal are not rounded and do not contain yeast, yeast fragments, intracellular vacuoles, or phagolysosomes (Figure 4B, lower panel). Since microglial cells did not express markers of alternative activation, we wished to determine whether they express IL-4Rα, which is essential for alternative activation of macrophages (Figure 5).[22] To approach this question, CD11b$^+$CD45^{high} macrophages and CD11b$^+$CD45^{dim} microglial cells of wild-type animals were stained for the presence of the IL-4Rα chain on their surface. Wild-type macrophages and microglial cells exhibited a median fluorescence intensity of 65.1, and 35.3, respectively. However, in IL-4R$\alpha^{-/-}$ macrophages and microglial cells used as negative controls, background median fluorescence intensity levels of 14.6 and 4.4, respectively, were found (data not shown). These results indicate that both cell types found in brains of infected susceptible wild-type mice express the IL-4Rα and, thus both cell types could be responsive to IL-4/IL-13. However, we did not detect any IL-4 and IL-13 protein in the brains of the mice of different genotypes examined by enzyme-linked immunosorbent assay (data not shown). Brain IL-4 production was also not detected by real-time PCR (Figure 6), while IL-13 was only detected at significant levels in the CNS of IL-13$^{T/+}$ mice. Since these cytokines were clearly expressed in the lungs of *Cryptococcus*-infected mice as shown previously,[19] we therefore conclude that macrophages are alternatively activated in the periphery (ie, lung), and enter the CNS subsequently. This cascade would explain why only macrophages, and not microglial cells, show an alternative activation status following i.n. infection of mice with *C. neoformans*. These data provide evidence in brains of mice for IL-4/IL-13-dependent alternatively activated macrophages, which are associated with uncontrolled infection.

Loss of Fungal Control in Mice Expressing IL-4 and IL-13 Is Associated with Development of aaMph

The development of aaMph has been shown to depend on IL-4 or IL-13.[22] To analyze whether aaMph found in susceptible wild-type mice (Figure 4) correlated with the presence of IL-4/IL-13, wild-type and Th2 mutant mice

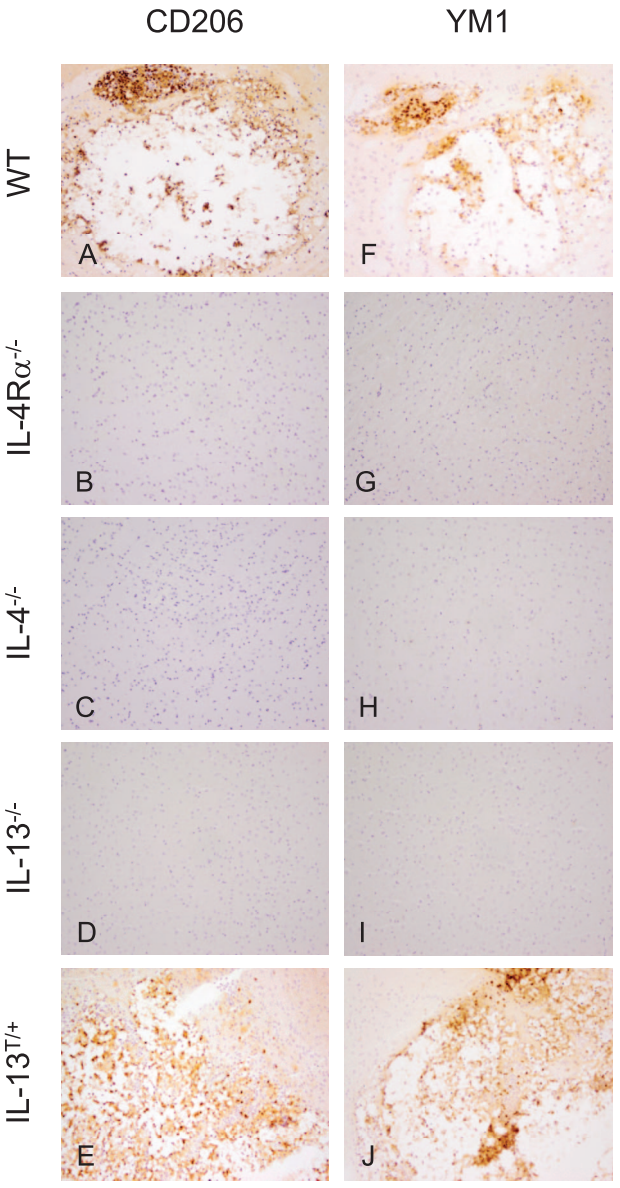

Figure 5. Alternatively activated macrophages develop in the CNS of susceptible wild-type, and IL-13$^{T/+}$ mice after i.n. infection with *C. neoformans*. **A–E:** Mannose receptor (CD206) expression as a marker for alternative activation of macrophages in the brain (60 dpi). In wild-type (WT) and IL-13$^{T/+}$ mice, macrophages show a strong expression of CD206, whereas the receptor is absent on cells of IL-4Rα$^{-/-}$ (**B**), IL-4$^{-/-}$ (**C**), and IL-13$^{-/-}$ (**D**) mice. In no case were microglial cells CD206 positive. Anti-CD206 immunostaining, magnification = original ×400. **F–J:** Chitinase YM1 expression as a marker for alternative activation of myeloid leukocytes in the brain (60 dpi). In wild-type and IL-13$^{T/+}$ mice, macrophages show a strong expression of YM1, whereas the molecule is absent in cells of IL-4Rα$^{-/-}$ (**G**), IL-4$^{-/-}$ (**H**), and IL-13$^{-/-}$ (**I**) mice. In no case microglial cells were YM1 positive. Anti-YM1 immunostaining; magnification = original ×400.

were compared for expression of CD206 and YM1. In wild-type mice large focal cystic lesions were tightly bordered by vacuolated voluminous macrophages, while in IL-13$^{T/+}$ mice these voluminous macrophages spread more diffusely into the adjacent CNS parenchyma (Figures 2A and 7A versus Figures 2E and 7E). In wild-type and IL-13$^{T/+}$ mice, these macrophages (Figure 7, A and E) express markers for aaMph, CD206, and YM1 (Figure 5, A, E, F, J). In contrast, in IL-4Rα$^{-/-}$, IL-4$^{-/-}$, and

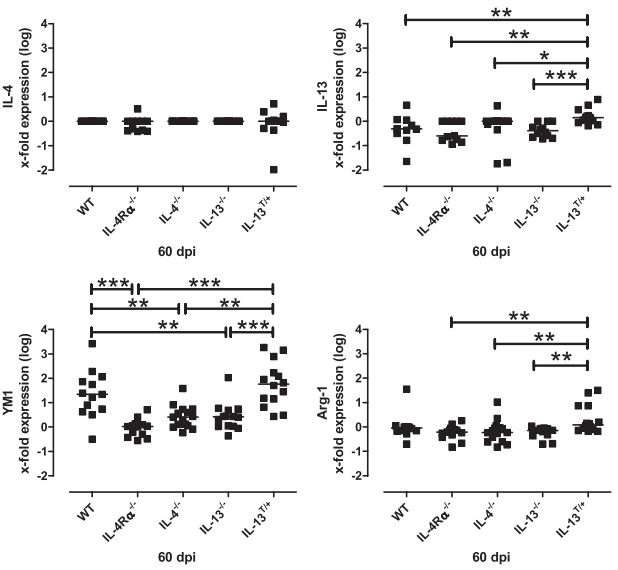

Figure 6. Differential transcription of IL-4, IL-13, YM1, and arginase-1 in wild-type, IL-4Rα$^{-/-}$, IL-4$^{-/-}$, IL-13$^{-/-}$, and IL-13$^{T/+}$ mice after i.n. infection with *C. neoformans*. YM1 mRNA expression in the brains of wild-type (WT) and IL-13$^{T/+}$ mice (60 dpi) was significantly elevated as compared with non-susceptible Th2 mutant mice. Arginase-1 mRNA expression in the brains of IL-13$^{T/+}$ mice (60 dpi) was significantly elevated as compared with non-susceptible Th2 mutant mice. No IL-4 expression was detected in the CNS of all genotypes. IL-13 expression was not detected in all genotypes except for IL-13$^{T/+}$ mice. Surprisingly, we detected some mRNA in IL-13 mutant mice using the primers described above, which results from the use of the IL-13 KO targeting vector.[35] Data from 8 to 12 representative mice per genotype are shown in the graph. Statistical analysis between wild-type, IL-4Rα$^{-/-}$, IL-4$^{-/-}$, IL-13$^{-/-}$, and IL-13$^{T/+}$ mice was performed by use of the Mann-Whitney-U Test, with: $^{*}P < 0.05$; $^{**}P < 0.01$, $^{***}P < 0.001$.

IL-13$^{-/-}$ mice (Figure 7, B–D), cells expressing YM1 or CD206, markers indicating IL-4/IL-13-dependent development of aaMph (Figure 5, B–D and G–I) were lacking. Further, microglial cells did not show markers of alternative activation in any of these genotypes. In the single mice that showed inflammatory foci among the resistant IL-4Rα$^{-/-}$, IL-4$^{-/-}$, IL-13$^{-/-}$ mice, no markers of alternative activation were detected either (supplemental Figure S2, A–F, see *http://ajp.amjpathol.org*).

Additional analysis of the alternative versus classical macrophage activation involved the detection of YM1 and arginase-1 mRNA by *real-time* PCR. In accordance with the immunohistochemical data showing cell-specific expression of high levels of YM1 at the protein level, significantly higher levels of YM1 mRNA were expressed in wild-type and IL-13$^{T/+}$ mice as compared with the non-susceptible genotypes. Arginase-1 mRNA was expressed at significantly higher levels in brains of infected IL-13$^{T/+}$ mice than in resistant mice. Low or no levels of YM1 and arginase-1 mRNA were expressed in IL-4Rα$^{-/-}$, IL-4$^{-/-}$, or IL-13$^{-/-}$ mice (Figure 6).

Microglial Cells Become Activated on Infection with C. neoformans *but, in Contrast to Macrophages, Do Not Contain Intracellular* C. neoformans

In the CNS, macrophages recruited from the periphery are important effector cells in cerebral *C. neoformans*

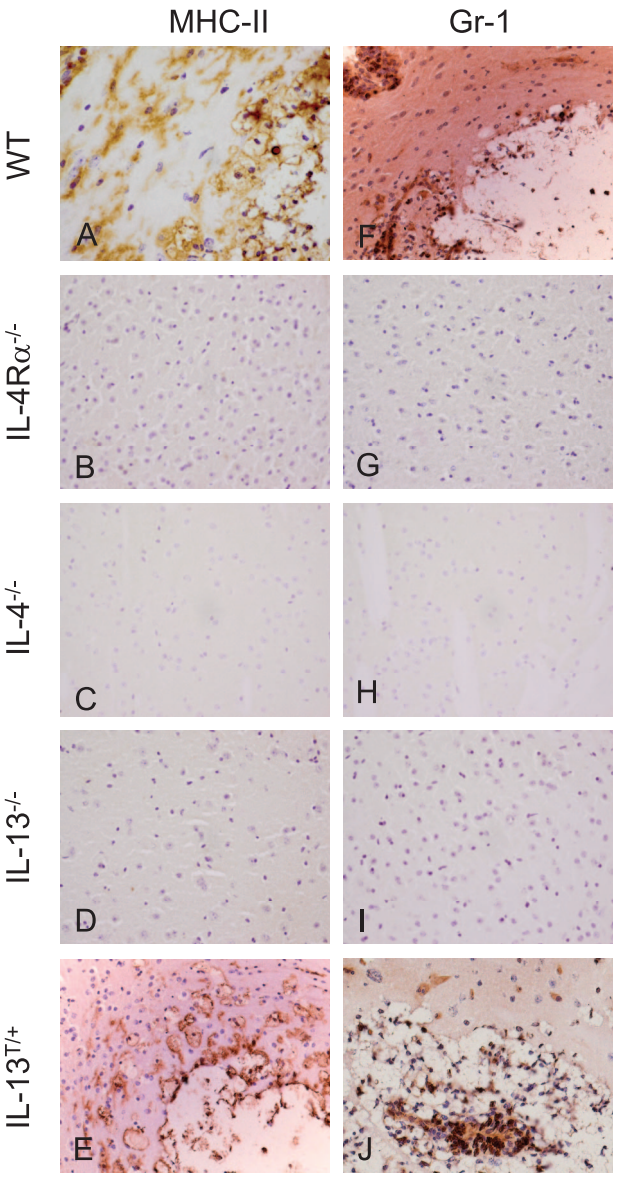

Figure 7. Innate cellular immune reaction pattern in wild-type, IL-4R$\alpha^{-/-}$, IL-4$^{-/-}$, IL-13$^{-/-}$, and IL-13$^{T/+}$ mice after i.n. infection with *C. neoformans*. **A–E:** In a BALB/c wild-type (WT) mouse (**A**), foamy rounded MHC class II$^+$ macrophages harboring yeast fragments are tightly bordering the lesion. In an IL-13$^{T/+}$ mice (**E**), voluminous macrophages harboring yeast fragments within their cytoplasm are demonstrated at the border of a pseudocystic lesion. In comparison with the wild-type (**A**), the lesion is less well demarcated by macrophages, which rather diffusely infiltrate the parenchyma. Microglial activation is a less prominent feature in an IL-13$^{T/+}$ mice, as compared with the wild-type (**A**). MHC class II$^+$ cells are generally absent in the CNS of IL-4R$^{-/-}$, IL-4$^{-/-}$, and IL-13$^{-/-}$ mice (**B–D**). Day 60 p.i.; Anti-MHC class II immunostaining; magnification = original ×400. **F–J:** In a BALB/c wild-type mouse (**F**), Gr-1$^+$ granulocytes are detected at the border and in the center of the lesion. Granulocytes also dissociate the vessel wall, which is localized at the **upper left**. In an Il-13$^{T/+}$ mice (**J**), many Gr-1$^+$ granulocytes are stained in the center and at the border of the lesion. Gr-1$^+$ cells are generally absent in the CNS of IL-4R$^{-/-}$, IL-4$^{-/-}$, and IL-13$^{-/-}$ mice (**G–I**). **F–J:** Day 60 p.i.; Anti-Gr-1 immunostaining; magnification = original ×400.

infection.[12,46–48] Moreover, expansion and proliferation of microglial cells is a crucial feature of a number of neuroinflammatory, traumatic, and neurodegenerative diseases.[49–52] In addition to F4/80$^+$ and MHC-II$^+$ macrophages, microglial cells were prominently activated in the vicinity of the lesions in *Cryptococcus*-infected wild-type mice (Figures 4A, 7A), whereas microglial activation was not as prominent in IL-13$^{T/+}$ mice (Figure 7E). By contrast, inflammatory leukocytes as stained by MHC class II or Gr-1 were generally absent in IL-4R$\alpha^{-/-}$, IL-4$^{-/-}$, or IL-13$^{-/-}$ mice (Figure 7, B–D, and G–I). In a single IL-4R$\alpha^{-/-}$ mouse, small microglial nodules and scarce Gr-1 positive cells were detected, but no round large or foamy macrophages were observed (supplemental Figure S3, A and D, see *http://ajp.amjpathol.org*). In two IL-4$^{-/-}$ mice, the granuloma consisted of compact F4/80$^+$ and MHC class II$^+$ macrophages and microglial cells (supplemental Figure S3B see *http://ajp.amjpathol.org*) as well as Gr-1$^+$ cells (supplemental Figure S3E see *http://ajp.amjpathol.org*), while multinucleated giant cells were absent and fibrous tissue as stained by Elastica van Gieson was not detected either (data not shown). A small fungal accumulation in a single IL-13$^{-/-}$ mouse was bordered by single F4/80$^+$ and MHC class II$^+$ macrophages, and discrete microglial cell activation was detected additionally (supplemental Figure S3C see *http://ajp.amjpathol.org*). Thus, microglial activation and some expansion occur in all of the infected brains following *C. neoformans* infection. However, microglial cells do not appear to contact and phagocytose cryptococci as macrophages do.

In agreement with the quantification presented in Figure 3, the highest numbers of granulocytes were detected in IL13$^{T/+}$ mice (Figure 7J). In wild-type mice some Gr-1$^+$ cells bordered the lesion and even infiltrated the CNS parenchyma (Figure 7F), while in IL-4R$\alpha^{-/-}$ and IL-4$^{-/-}$ mice that showed cryptococci in the brain, granulocytes were confined to the inflammatory focus and appeared at low numbers (supplemental Figure S3, D and E, see *http://ajp.amjpathol.org*). In one IL-13$^{-/-}$ mouse that showed cryptococcal infection of the brain, granulocytes were barely detectable by immunohistochemistry (supplemental Figure S3F, see *http://ajp.amjpathol.org*), consistent with the data generated by flow cytometry analysis (data not shown). Thus, in addition to aaMph, granulocytes are also detectable in the brains of susceptible genotypes during cryptococcal infection.

Discussion

In the present study, we analyzed the roles of the Th2 cytokines IL-4 and IL-13 in cerebral cryptococcosis following intranasal infection, and found that mice defective in one or both cytokines were largely resistant to the infection. These mice harbored low or no fungi within their brains, and recruited low numbers of leukocytes. In rare cases of infection of their brains, they developed lesions characterized by a classical cellular immune response such as microglial nodules or granuloma formation. In contrast, susceptible wild-type and IL-13 transgenic BALB/c mice harbored high fungal burdens leading to lesion morphology, characterized by a pseudocystic appearance disseminated throughout the brain parenchyma. Most importantly, these inflammatory foci are characterized by large aaMph expressing CD206, YM1,

and arginase-1 and containing fungi. These cells appear in abundance and border the lesions. Activated microglial cells were also found at high numbers, but these cells did not express markers of alternative activation nor did they contain fungi. Collectively this shows that development of aaMph in the CNS after pulmonary *C. neoformans* infection and dissemination to the CNS is crucially dependent on IL-4 and IL-13, and these macrophages are unable to control cerebral fungal growth. Conversely, no aaMph developed in the absence of IL-4 and/or IL-13. Also, neither morphologically resting nor activated microglia did show any expression of markers typical of alternative activation (neither CD206 nor YM1).

Cerebral cryptococcosis in *C. neoformans*-infected BALB/c mice is characterized by both the production of Th1 and Th2 cytokines. Th1 cytokines such as interferon-γ, IL-12 and tumor necrosis factor have been demonstrated to be crucially involved in protection from lethal cryptococcosis.[17–19,53–55] However, in a model of cerebral cryptococcosis Maffei et al[43] did not describe a polarization of Th1 or Th2 responses by detecting transcripts of tumor necrosis factor and inducible nitric oxide synthase in addition to IL-4, and IL-10. Others propose that Th1 cytokines are of prime importance since expression of these factors correlates with protection against *C. neoformans* in the CNS, whereas Th2 cytokines were not elevated in a murine model of *C. neoformans* infection of the CNS with a prior peripheral immunization.[55,56] Huffnagle et al stated that the host defense mechanisms that clear *C. neoformans* from the CNS appear to be similar to those in the lungs[17] ie, via a Th1 cell-mediated inflammatory response, and that Th2 type immunity is ineffective at eliminating the infection in the brain and results in decreased survival. Extending these results, we show that Th2 cytokines highly impact the inflammatory response that develops within the CNS by altering macrophage activation. Overexpression of IL-13 in IL-13$^{T/+}$ mice leads to the most severe inflammatory phenotype with the highest fungal burdens, highest frequency of CNS involvement following pulmonary infection, largest inflammatory foci, poor demarcation by macrophages at the lesion border, and highest numbers of leukocytes infiltrating the parenchyma. These findings were in contrast to Olszewski et al who used the *C. neoformans* strain (serotype A) H99 in a model of intratracheal infection in C57BL/6 × 129 F2 mice.[12] Olszewski et al showed that the intracranial inflammatory response after transcapillary invasion of the fungi was minimal without local leukocyte accumulation, and only scarce neutrophils were detected at 4–6 weeks post infection. Interestingly these authors did not mention any macrophages in their model of cerebral cryptococcosis. These differences in the immune response of wild-type animals in comparison with the results presented here may be due to differences in the cryptococcal strain and also the host genetic background.

Microglial cell activation and expansion was observed not only in susceptible genotypes, but also in resistant IL-4$^{-/-}$ and IL-4Rα$^{-/-}$ mice, where, although in rare cases, these hosts showed microglial cell activation and expansion with a highly specific morphological pattern. Studying the role of microglial cells in cerebral cryptococcosis *in vitro*, using human fetal microglial cultures, Lee et al[57] showed that microglial cells initially internalized, and contained yeasts within phagolysosomes. Yeast were observed growing extracellularly 16 to 24 hours after being phagocytosed.[57] Based on morphological analysis, the authors differentiated between two types of phagosomes in microglia: spacious phagosomes and close-fitting phagosomes, and suggest that in human microglia, *C. neoformans* survive and replicate within spacious phagosomes. This study was undertaken *in vitro* and with human fetal microglia cells that on stimulation with *C. neoformans*, may have differentiated into phagocytes. We believe that this may be the first thorough description of aaMph, and not genuine microglial cells, in cerebral cryptococcosis, although the concept of different macrophage activation status[58,59] had not been put forward yet. *In vitro* and *in vivo* observations on *C. neoformans* interaction with alveolar macrophages were demonstrated to be critical for containing the infection via a unique intracellular pathogenic strategy involving cytoplasmic accumulation of polysaccharide-containing vesicles and intracellular replication leading to the formation of spacious phagosomes in which multiple cryptococcal cells are present.[60–62] Reports on the alternative activation status of these alveolar macrophages in the context of Th2-mediated immune responses in bronchopulmonary cryptococcosis have pointed out their unique roles in disease.[19,44]

Markers of alternative activation have been studied in CNS diseases only recently. For example, in a mouse model of Alzheimer disease, YM1 mRNA was reported to increase, and in the brains of Alzheimer patients chitinase 3-like-1 and -2 mRNA levels were significantly elevated, although the exact cellular source of the increased transcription of these markers was not determined.[63] In an experimental autoimmune encephalomyelitis model, microglial cells in the resting and the activated state were shown to produce YM1 and lacked the production of NO in an IL-4-dependent manner. Using bone marrow chimeras, the authors concluded that macrophages entering the CNS from the periphery exhibit a dual phenotype (classical Mph as well as aaMph) since these cells, in contrast to microglial cells, also produced inducible nitric oxide synthase.[64] Interestingly these authors found YM1 mRNA in resting microglia, and YM1 expression as measured by fluorescence-activated cell sorting analysis in CD45^{low} and CD45^{high} expressing 'microglia' and in peripheral macrophages. In our study CD11b^{+}CD45^{high} expressing cells were interpreted as macrophages according to the original description of this technique,[41,65] and we did not detect YM1 expression by immunohistochemistry on resting or activated microglial cells in susceptible mice. Because of the obstacle of differentiating *in situ* between blood-derived macrophages entering the inflamed CNS and microglial cells solely by immunohistochemical techniques, we have added fluorescence-activated cell sorting analysis and ultrastructural analysis to strengthen our findings. In agreement with our results, Ponomarev et al were unable to detect YM1 expression in IL-4- or IL-4Rα- deficient mice.[64] Since we did not detect

any IL-4 and IL-13 protein or mRNA in the CNS of wild-type mice infected with *C. neoformans*, we believe that macrophages are alternatively activated in the periphery (ie, the lung), and this may be the reason why only macrophages, and not microglial cells show an alternative activation status.

We believe that it is of utmost importance to dissect the function and morphology of macrophages and microglial cells in cerebral cryptococcosis in particular in view of possible differences in immune reactions from individuals with differing susceptibility. Shibuya et al have examined the morphological characteristics of macrophages in bronchopulmonary cryptococcosis in immunocompetent individuals,[66] in patients with AIDS, and in patients undergoing highly active antiretroviral therapy (HAART). They found that immunodeficiency was associated with histiocytic, minor lymphocytic and granulocytic response, while HAART induces a massive histiocytic and lymphocytic involvement. In a murine model of cerebral cryptococcosis using i.v. infection with a human isolate Chretien et al localized the fungi to mononuclear cells in cerebrovascular capillaries, in endothelial cells and in vacuolated macrophages within the CNS parenchyma in cystic lesions.[10] Furthermore, a reaction pattern in HIV-negative patients similar to mice recovering from cryptococcosis with a granulomatous pattern was also described.[10] Our results show a strict IL-4- and IL-13-dependency of macrophage frequency, morphology, and functional status leading to distinct lesion morphology. Our data in non-susceptible IL-4- and IL-4Rα-deficient mice also point to a protective granulomatous reaction pattern, which may be an interesting model to further study subtle protective genetically determined effects in cerebral cryptococcosis.

Acknowledgments

We thank Dr. Arturo Casadevall for generously providing mAb anti-GXM. Meike Brenkmann, Cordula Westermann, Alexandra Förster, and Juliane Richter are very kindly acknowledged for expert technical assistance.

References

1. Mitchell TG, Perfect JR: Cryptococcosis in the era of AIDS–100 years after the discovery of Cryptococcus neoformans. Clin Microbiol Rev 1995, 8:515–548
2. Lortholary O, Nunez H, Brauner MW, Dromer F: Pulmonary cryptococcosis. Semin Respir Crit Care Med 2004, 25:145–157
3. Malik R, Krockenberger MB, Cross G, Doneley R, Madill DN, Black D, McWhirter P, Rozenwax A, Rose K, Alley M, Forshaw D, Russell-Brown I, Johnstone AC, Martin P, O'Brien CR, Love DN: Avian cryptococcosis. Med Mycol 2003, 41:115–124
4. McAdams HP, Rosado-de-Christenson ML, Lesar M, Templeton PA, Moran CA: Thoracic mycoses from endemic fungi: radiologic-pathologic correlation. Radiographics 1995, 15:255–270
5. McAdams HP, Rosado-de-Christenson ML, Templeton PA, Lesar M, Moran CA: Thoracic mycoses from opportunistic fungi: radiologic-pathologic correlation. Radiographics 1995, 15:271–286
6. Decken K, Kohler G, Palmer-Lehmann K, Wunderlin A, Mattner F, Magram J, Gately MK, Alber G: Interleukin-12 is essential for a protective Th1 response in mice infected with Cryptococcus neoformans. Infect Immun 1998, 66:4994–5000
7. Goldman D, Cho Y, Zhao M, Casadevall A, Lee SC: Expression of inducible nitric oxide synthase in rat pulmonary Cryptococcus neoformans granulomas. Am J Pathol 1996, 148:1275–1282
8. Huffnagle GB, Lipscomb MF, Lovchik JA, Hoag KA, Street NE: The role of CD4+ and CD8+ T cells in the protective inflammatory response to a pulmonary cryptococcal infection. J Leukoc Biol 1994, 55:35–42
9. Retini C, Kozel TR, Pietrella D, Monari C, Bistoni F, Vecchiarelli A: Interdependency of interleukin-10 and interleukin-12 in regulation of T-cell differentiation and effector function of monocytes in response to stimulation with Cryptococcus neoformans. Infect Immun 2001, 69:6064–6073
10. Chretien F, Lortholary O, Kansau I, Neuville S, Gray F, Dromer F: Pathogenesis of cerebral Cryptococcus neoformans infection after fungemia. J Infect Dis 2002, 186:522–530
11. Lortholary O, Improvisi L, Nicolas M, Provost F, Dupont B, Dromer F: Fungemia during murine cryptococcosis sheds some light on pathophysiology. Med Mycol 1999, 37:169–174
12. Olszewski MA, Huffnagle GB, McDonald RA, Lindell DM, Moore BB, Cook DN, Toews GB: The role of macrophage inflammatory protein-1 alpha/CCL3 in regulation of T cell-mediated immunity to Cryptococcus neoformans infection. J Immunol 2000, 165:6429–6436
13. Koguchi Y, Kawakami K: Cryptococcal infection and Th1-Th2 cytokine balance. Int Rev Immunol 2002, 21:423–438
14. McKenzie AN, Zurawski G: Interleukin-13: characterization and biologic properties. Cancer Treat Res 1995, 80:367–378
15. Blackstock R, Murphy JW: Role of interleukin-4 in resistance to Cryptococcus neoformans infection. Am J Respir Cell Mol Biol 2004, 30:109–117
16. Kawakami K, Hossain Qureshi M, Zhang T, Koguchi Y, Xie Q, Kurimoto M, Saito A: Interleukin-4 weakens host resistance to pulmonary and disseminated cryptococcal infection caused by combined treatment with interferon-gamma-inducing cytokines. Cell Immunol 1999, 197:55–61
17. Huffnagle GB, McNeil LK: Dissemination of C. neoformans to the central nervous system: role of chemokines. Th1 immunity and leukocyte recruitment. J Neurovirol 1999, 5:76–81
18. Arora S, Hernandez Y, Erb-Downward JR, McDonald RA, Toews GB, Huffnagle GB: Role of IFN-gamma in regulating T2 immunity and the development of alternatively activated macrophages during allergic bronchopulmonary mycosis. J Immunol 2005, 174:6346–6356
19. Müller U, Stenzel W, Köhler G, Werner C, Polte T, Hansen G, Schutze N, Straubinger RK, Blessing M, McKenzie AN, Brombacher F, Alber G: IL-13 induces disease-promoting type 2 cytokines, alternatively activated macrophages and allergic inflammation during pulmonary infection of mice with Cryptococcus neoformans. J Immunol 2007, 179:5367–5377
20. Nathan C, Shiloh MU: Reactive oxygen and nitrogen intermediates in the relationship between mammalian hosts and microbial pathogens. Proc Natl Acad Sci USA 2000, 97:8841–8848
21. Stein M, Keshav S, Harris N, Gordon S: Interleukin 4 potently enhances murine macrophage mannose receptor activity: a marker of alternative immunologic macrophage activation. J Exp Med 1992, 176:287–292
22. Gordon S: Alternative activation of macrophages. Nat Rev Immunol 2003, 3:23–35
23. Mosser DM: The many faces of macrophage activation. J Leukoc Biol 2003, 73:209–212
24. Lumeng CN, Bodzin JL, Saltiel AR: Obesity induces a phenotypic switch in adipose tissue macrophage polarization. J Clin Invest 2007, 117:175–184
25. Lumeng CN, Deyoung SM, Bodzin JL, Saltiel AR: Increased inflammatory properties of adipose tissue macrophages recruited during diet-induced obesity. Diabetes 2007, 56:16–23
26. Herbert DR, Holscher C, Mohrs M, Arendse B, Schwegmann A, Radwanska M, Leeto M, Kirsch R, Hall P, Mossmann H, Claussen B, Forster I, Brombacher F: Alternative macrophage activation is essential for survival during schistosomiasis and downmodulates T helper 1 responses and immunopathology. Immunity 2004, 20:623–635
27. Pesce J, Kaviratne M, Ramalingam TR, Thompson RW, Urban JF, Jr., Cheever AW, Young DA, Collins M, Grusby MJ, Wynn TA: The IL-21 receptor augments Th2 effector function and alternative macrophage activation. J Clin Invest 2006, 116:2044–2055

28. Holcomb IN, Kabakoff RC, Chan B, Baker TW, Gurney A, Henzel W, Nelson C, Lowman HB, Wright BD, Skelton NJ, Frantz GD, Tumas DB, Peale FV, Jr., Shelton DL, Hebert CC: FIZZ1, a novel cysteine-rich secreted protein associated with pulmonary inflammation, defines a new gene family. EMBO J 2000, 19:4046–4055
29. Hesse M, Modolell M, La Flamme AC, Schito M, Fuentes JM, Cheever AW, Pearce EJ, Wynn TA: Differential regulation of nitric oxide synthase-2 and arginase-1 by type 1/type 2 cytokines in vivo: granulomatous pathology is shaped by the pattern of L-arginine metabolism. J Immunol 2001, 167:6533–6544
30. Stutz AM, Pickart LA, Trifilieff A, Baumruker T, Prieschl-Strassmayr E, Woisetschlager M: The Th2 cell cytokines IL-4 and IL-13 regulate found in inflammatory zone 1/resistin-like molecule alpha gene expression by a STAT6 and CCAAT/enhancer-binding protein-dependent mechanism. J Immunol 2003, 170:1789–1796
31. Prasse A, Pechkovsky DV, Toews GB, Jungraithmayr W, Kollert F, Goldmann T, Vollmer E, Muller-Quernheim J, Zissel G: A vicious circle of alveolar macrophages and fibroblasts perpetuates pulmonary fibrosis via CCL18. Am J Respir Crit Care Med 2006, 173:781–792
32. Hölscher C, Arendse B, Schwegmann A, Myburgh E, Brombacher F: Impairment of alternative macrophage activation delays cutaneous leishmaniasis in nonhealing BALB/c mice. J Immunol 2006, 176: 1115–1121
33. Mohrs M, Ledermann B, Köhler G, Dorfmuller A, Gessner A, Brombacher F: Differences between IL-4- and IL-4 receptor alpha-deficient mice in chronic leishmaniasis reveal a protective role for IL-13 receptor signaling. J Immunol 1999, 162:7302–7308
34. Kopf M, Le Gros G, Bachmann M, Lamers MC, Bluethmann H, Kohler G: Disruption of the murine IL-4 gene blocks Th2 cytokine responses. Nature 1993, 362:245–248
35. McKenzie GJ, Bancroft A, Grencis RK, McKenzie AN: A distinct role for interleukin-13 in Th2-cell-mediated immune responses. Curr Biol 1998, 8:339–342
36. Emson CL, Bell SE, Jones A, Wisden W, McKenzie AN: Interleukin (IL)-4-independent induction of immunoglobulin (Ig)E, and perturbation of T cell development in transgenic mice expressing IL-13. J Exp Med 1998, 188:399–404
37. Stenzel W, Soltek S, Miletic H, Hermann MM, Körner H, Sedgwick JD, Schluter D, Deckert M: An essential role for tumor necrosis factor in the formation of experimental murine Staphylococcus aureus-induced brain abscess and clearance. J Neuropathol Exp Neurol 2005, 64:27–36
38. Livak KJ, Schmittgen TD: Analysis of relative gene expression data using real-time quantitative PCR and the 2(-Delta Delta C[T]) Method. Methods 2001, 25:402–408
39. Ford AL, Goodsall AL, Hickey WF, Sedgwick JD: Normal adult ramified microglia separated from other central nervous system macrophages by flow cytometric sorting. Phenotypic differences defined and direct ex vivo antigen presentation to myelin basic protein-reactive CD4+ T cells compared. J Immunol 1995, 154:4309–4321
40. Stenzel W, Dahm J, Sanchez-Ruiz M, Miletic H, Hermann M, Courts C, Schwindt H, Utermöhlen O, Schluter D, Deckert M: Regulation of the inflammatory response to Staphylococcus aureus-induced brain abscess by interleukin-10. J Neuropathol Exp Neurol 2005, 64:1046–1057
41. Sedgwick JD, Ford AL, Foulcher E, Airriess R: Central nervous system microglial cell activation and proliferation follows direct interaction with tissue-infiltrating T cell blasts. J Immunol 1998, 160:5320–5330
42. Shao X, Mednick A, Alvarez M, van Rooijen N, Casadevall A, Goldman DL: An innate immune system cell is a major determinant of species-related susceptibility differences to fungal pneumonia. J Immunol 2005, 175:3244–3251
43. Maffei CM, Mirels LF, Sobel RA, Clemons KV, Stevens DA: Cytokine and inducible nitric oxide synthase mRNA expression during experimental murine cryptococcal meningoencephalitis. Infect Immun 2004, 72:2338–2349
44. Chen GH, Olszewski MA, McDonald RA, Wells JC, Paine R, 3rd, Huffnagle GB, Toews GB: Role of granulocyte macrophage colony-stimulating factor in host defense against pulmonary Cryptococcus neoformans infection during murine allergic bronchopulmonary mycosis. Am J Pathol 2007, 170:1028–1040
45. Milam JE, Herring-Palmer AC, Pandrangi R, McDonald RA, Huffnagle GB, Toews GB: Modulation of the Pulmonary T2 Response to Cryptococcus neoformans by Intratracheal Delivery of a TNF{alpha}-expressing Adenoviral Vector. Infect Immun 2007, 75:4951–4958
46. Blasi E, Barluzzi R, Mazzolla R, Mosci P, Bistoni F: Experimental model of intracerebral infection with Cryptococcus neoformans: roles of phagocytes and opsonization. Infect Immun 1992, 60:3682–3688
47. Goldman DL, Casadevall A, Cho Y, Lee SC: Cryptococcus neoformans meningitis in the rat. Lab Invest 1996, 75:759–770
48. Lee SC, Dickson DW, Casadevall A: Pathology of cryptococcal meningoencephalitis: analysis of 27 patients with pathogenetic implications. Hum Pathol 1996, 27:839–847
49. Babcock AA, Wirenfeldt M, Holm T, Nielsen HH, Dissing-Olesen L, Toft-Hansen H, Millward JM, Landmann R, Rivest S, Finsen B, Owens T: Toll-like receptor 2 signaling in response to brain injury: an innate bridge to neuroinflammation. J Neurosci 2006, 26:12826–12837
50. Ladeby R, Wirenfeldt M, Garcia-Ovejero D, Fenger C, Dissing-Olesen L, Dalmau I, Finsen B: Microglial cell population dynamics in the injured adult central nervous system. Brain Res Brain Res Rev 2005, 48:196–206
51. Nguyen MD, Julien JP, Rivest S: Innate immunity: the missing link in neuroprotection and neurodegeneration? Nat Rev Neurosci 2002, 3:216–227
52. Stenzel W, Soltek S, Sanchez-Ruiz M, Akira S, Miletic H, Schluter D, Deckert M: Both TLR2 and TLR4 are required for the effective immune response in Staphylococcus aureus-induced experimental murine brain abscess. Am J Pathol 2008, 172:132–145
53. Hernandez Y, Arora S, Erb-Downward JR, McDonald RA, Toews GB, Huffnagle GB: Distinct roles for IL-4 and IL-10 in regulating T2 immunity during allergic bronchopulmonary mycosis. J Immunol 2005, 174:1027–1036
54. Kleinschek MA, Müller U, Brodie SJ, Stenzel W, Kohler G, Blumenschein WM, Straubinger RK, McClanahan T, Kastelein RA, Alber G: IL-23 enhances the inflammatory cell response in Cryptococcus neoformans infection and induces a cytokine pattern distinct from IL-12. J Immunol 2006, 176:1098–1106
55. Zhou Q, Gault RA, Kozel TR, Murphy WJ: Protection from direct cerebral cryptococcus infection by interferon-gamma-dependent activation of microglial cells. J Immunol 2007, 178:5753–5761
56. Uicker WC, Doyle HA, McCracken JP, Langlois M, Buchanan KL: Cytokine and chemokine expression in the central nervous system associated with protective cell-mediated immunity against Cryptococcus neoformans. Med Mycol 2005, 43:27–38
57. Lee SC, Kress Y, Zhao ML, Dickson DW, Casadevall A: Cryptococcus neoformans survive and replicate in human microglia. Lab Invest 1995, 73:871–879
58. Edwards JP, Zhang X, Frauwirth KA, Mosser DM: Biochemical and functional characterization of three activated macrophage populations. J Leukoc Biol 2006, 80:1298–1307
59. Taylor PR, Martinez-Pomares L, Stacey M, Lin HH, Brown GD, Gordon S: Macrophage receptors and immune recognition. Annu Rev Immunol 2005, 23:901–944
60. Alvarez M, Casadevall A: Phagosome extrusion and host-cell survival after Cryptococcus neoformans phagocytosis by macrophages. Curr Biol 2006, 16:2161–2165
61. Feldmesser M, Tucker S, Casadevall A: Intracellular parasitism of macrophages by Cryptococcus neoformans. Trends Microbiol 2001, 9:273–278
62. Tucker SC, Casadevall A: Replication of Cryptococcus neoformans in macrophages is accompanied by phagosomal permeabilization and accumulation of vesicles containing polysaccharide in the cytoplasm. Proc Natl Acad Sci USA 2002, 99:3165–3170
63. Colton CA, Mott RT, Sharpe H, Xu Q, Van Nostrand WE, Vitek MP: Expression profiles for macrophage alternative activation genes in AD and in mouse models of AD. J Neuroinflammation 2006, 3:27
64. Ponomarev ED, Maresz K, Tan Y, Dittel BN: CNS-derived interleukin-4 is essential for the regulation of autoimmune inflammation and induces a state of alternative activation in microglial cells. J Neurosci 2007, 27:10714–10721
65. Dick AD, Ford AL, Forrester JV, Sedgwick JD: Flow cytometric identification of a minority population of MHC class II positive cells in the normal rat retina distinct from CD45lowCD11b/c+CD4low parenchymal microglia. Br J Ophthalmol 1995, 79:834–840
66. Shibuya K, Hirata A, Omuta J, Sugamata M, Katori S, Saito N, Murata N, Morita A, Takahashi K, Hasegawa C, Mitsuda A, Hatori T, Nonaka H: Granuloma and cryptococcosis. J Infect Chemother 2005, 11:115–122